



CHARACTERIZATION AND COMPARISON OF $\text{Al}_{0.22}\text{Ga}_{0.78}\text{As}/\text{In}_{0.2}\text{Ga}_{0.8}\text{As}$ AND $\text{In}_{0.49}\text{Ga}_{0.51}\text{P}/\text{Al}_{0.24}\text{Ga}_{0.76}\text{As}/\text{In}_{0.2}\text{Ga}_{0.8}\text{As}$ PHEMT FOR DIFFERENT GATE LENGTHS

Rini Lahiri[†] and Ricky Anthony^{*}

[†]Department Of Electronics and Communication Engineering National Institute of Technology-Nagaland

^{*}Department Of Electronics and Communication Engineering Heritage Institute of Technology, Kolkata
Silchar, India

rini.lahiri16@gmail.com

ABSTRACT

The paper represents a simulative study of band structure, drain-characteristics, transfer characteristics and transconductance of the conventional AlGaAs/AlGaAs/InGaAs pseudomorphic high-electron-mobility-transistors (PHEMT) which was improved by using double δ -doped layers of 1nm each and to obtain a transconductance of 454 mS/mm for 0.5 μm gate length. A further improvement was achieved in the linearity of the device, by replacing the AlGaAs barrier layer by an InGaP material and transconductance of 483 mS/mm. Both the PHEMTs with δ -doped layers are further studied for different gate lengths (L_g). The improved G_m and I_d - V_d have been analyzed and discussed for variable gate lengths (L_g) to provide an optimized result.

Keywords: pseudomorphic HEMT, TCAD; 2-DEG, δ -doping; InGaP layer, transconductance, gate length scaling.

Received 23-06-2012, revised 28-06-2012, online 03-07-2012

I. INTRODUCTION

The physics of semiconductor heterojunction have proved to be a very useful device building block for many advanced devices in the history of semiconductor industry. For high-power and high-frequency integrated circuit applications, heterostructure field-effect transistors (HFETs) and heterostructure bipolar transistors (HBTs) have been widely studied [1]. The high electron mobility transistor (HEMT) has become the most upcoming topic in research because of the presence of two dimensional electron gas (2DEG) at the interface formed due the conduction-band and valence-band discontinuities and hence the increase of mobility of electrons through the channel [2].

In 1986, the conventional GaAs pseudomorphic HEMT (PHEMT) i.e GaAs/AlGaAs/InGaAs/GaAs HEMT was introduced as an alternative to the AlGaAs/GaAs HEMT. Since studies showed that AlGaAs material system suffered from problems related to shift in voltage threshold and drain current-voltage (I-V) saturation collapse, InGaAs material, which showed high mobility and strong electron confinement, was used as the channel material.

Again, when compared with the conventional homogeneously doped pseudomorphic high-electron mobility transistor (PHEMT) structures, the δ -doped PHEMT structures have showed several advantages. A δ -doped layer (planar doped/pulse doped/atomic doped) is a monolayer of 0.5nm-1nm (atomic dimension) and is used above the spacer layer to obtain high sheet charge density. The research have showed that δ -doped PHEMT has higher breakdown voltage, higher 2DEG carrier density, higher intrinsic transconductance, better control of the threshold voltage and improved linearity on

PHEMT I-V transfer characteristics than the conventional PHEMT [3]. Submicron InAlN/GaN HEMT have also been reported to provide high I_{ds} (drain to source current) of 2.5A/mm and transconductance of 600mS/mm with a cutoff frequency of 150GHz [4]. GaN based HEMT devices have also been studied in the last decade in terms of analytical models and characteristics [5].

Moreover, the use of InGaP material as barrier layer increases the performance of the PHEMT. The crystal quality of InGaP material is very high and it has a high bandgap which reduces 1/f noise and Gunn oscillation effect. Studies have also shown that the etching selectivity between the InGaP and GaAs is excellent which increases the device manufacturability.

In this paper we have shown using Silvaco (ATLAS) TCAD simulation tool, that how the performance of an AlGaAs /AlGaAs /InGaAs/ GaAs changes with delta-doping and different gate lengths and, how it can be improved by replacing the AlGaAs barrier layer by an InGaP barrier layer. The InGaP/AlGaAs/InGaAs structure increases the conduction band discontinuity between the spacer and the channel layer which improves the carrier confinement and provides high current density [6], [7]. The Hall mobility of this structure is high due to smoothness of the AlGaAs / InGaAs interface [8].

II. DEVICE STRUCTURE

The Table I shows the layers and the x-compositions for all the three PHEMT devices which have been studied in this paper. The structure I is a simple AlGaAs/InGaAs/GaAs

PHEMT without any delta doping. This device is modified using double delta doping layers as shown in structure II, to increase the carrier confinement. To further improve the performance of the device, the $Al_xGa_{1-x}As$ layer is replaced by an $In_{1-x}Ga_xP$ layer, as shown in the structure III. The Table II shows the respective doping and the thicknesses of the layers used in the devices.

For HEMT, the quality of material is very important for optimal device performance and can get degraded very easily by impurities, defects, hetero-interface roughness and lattice mismatch strain. To overcome this problem, slow growth rates of 1 to 2 atomic layers per second i.e epitaxial growth of lattice matched materials on heated semi-insulating GaAs is done. The methods of molecular beam epitaxy (MBE) or metal-organic chemical vapour deposition (MOCVD) are employed to obtain this epitaxial growth [9].

Table I. The Layers And Their Respective X-Compositions Used In The Simulation Study

Device Layers	[Structure I] AlGaAs/AlGaAs/ InGaAs PHEMT without δ -doping	[Structure II] AlGaAs/AlGaAs/ InGaAs PHEMT	[Structure III] InGaP/AlGaAs/ InGaAs PHEMT
Cap	GaAs	GaAs	GaAs
Barrier	$Al_xGa_{1-x}As$ ($x=0.22$)	$Al_xGa_{1-x}As$ ($x=0.22$)	$In_{1-x}Ga_xP$ ($x=0.51$)
Delta 1	-	$Al_xGa_{1-x}As$ ($x=0.22$)	$Al_xGa_{1-x}As$ ($x=0.24$)
Spacer 1	$Al_xGa_{1-x}As$ ($x=0.22$)	$Al_xGa_{1-x}As$ ($x=0.22$)	$Al_xGa_{1-x}As$ ($x=0.24$)
Channel	$In_{1-x}Ga_xAs$ ($x=0.8$)	$In_{1-x}Ga_xAs$ ($x=0.8$)	$In_{1-x}Ga_xAs$ ($x=0.8$)
Spacer 2	-	$Al_xGa_{1-x}As$ ($x=0.22$)	$Al_xGa_{1-x}As$ ($x=0.24$)
Delta 2	-	$Al_xGa_{1-x}As$ ($x=0.22$)	$Al_xGa_{1-x}As$ ($x=0.24$)
Layer on buffer	-	$Al_xGa_{1-x}As$ ($x=0.22$)	$Al_xGa_{1-x}As$ ($x=0.24$)
Buffer	GaAs	GaAs	GaAs

Table II. The Thickness And The Doping concentration Of All The Layers Of The Devices Used in The Simulation Study

Device Layers	[Structure I] AlGaAs/AlGaAs/ InGaAs PHEMT without δ -doping		[Structure II] AlGaAs/AlGaAs/ InGaAs PHEMT		[Structure III] InGaP/AlGaAs/ InGaAs PHEMT	
	T (nm)	n (cm^{-3})	T (nm)	n (cm^{-3})	T (nm)	n (cm^{-3})
Cap	50	2×10^{19}	50	2×10^{19}	50	2×10^{19}
Barrier	30	8×10^{17}	30	undoped	30	undoped
Delta 1	-	-	1	-	1	-
Spacer 1	4	-	3	-	3	-
Channel	14	-	14	-	14	-
Spacer 2	-	-	3	-	3	-
Delta 2	-	-	1	-	1	-
Layer on buffer	-	-	38	-	38	-
Buffer	302	-	360	-	360	-

T = thickness of a layer & n = n-type doping concentration

III. RESULTS AND DISCUSSIONS

The simple AlGaAs/ AlGaAs/ InGaAs device (without δ -doped layer) of $0.5\mu m$ gate length was simulated using Silvaco ATLAS simulator. The Fig.1 is the band diagram of the device showing the formation 2-DEG triangular well in the channel layer. The lowest potential is obtained at $-0.054V$.

The band diagrams for AlGaAs/AlGaAs/InGaAs PHEMT and InGaP/AlGaAs/InGaAs PHEMT both with δ -doped layer are shown in Fig.2 and Fig.3 respectively. Both the structures show the formation of rectangular well due to double δ -doped layers increasing the electron carrier confinement. Moreover, the lowest potential level obtained is $-0.058V$ for AlGaAs/AlGaAs/InGaAs PHEMT with δ -doping, which is increased to $-0.078V$ when AlGaAs barrier layer is replaced by InGaP layer.

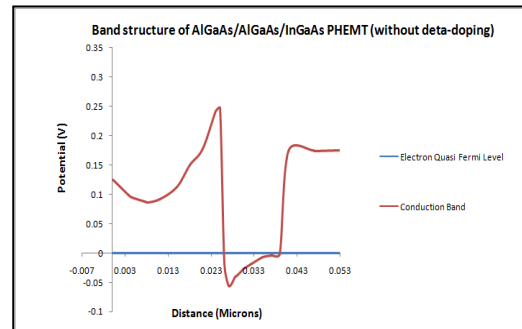


Figure 1: Band Diagram of AlGaAs/AlGaAs/InGaAs PHEMT without δ -doping.

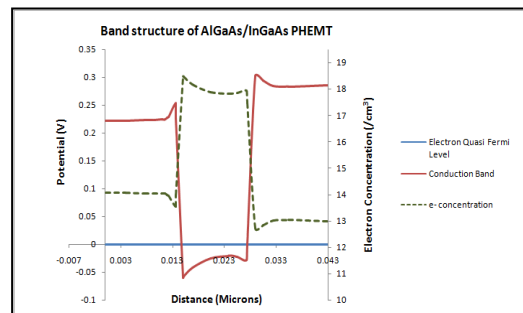


Figure 2: Band Diagram of AlGaAs/AlGaAs/InGaAs PHEMT with δ -doping.

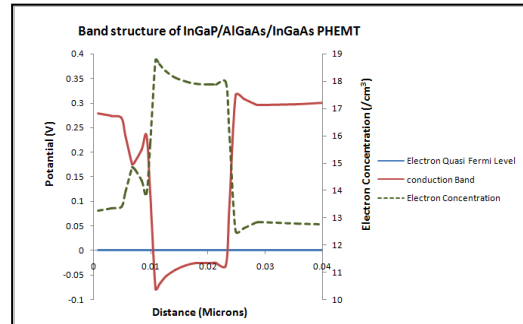


Figure 3: Band Diagram of InGaP/AlGaAs/InGaAs PHEMT with δ -doping.

The drain characteristics and the transfer characteristics for all the three device structures are studied for $0.5\mu m$ gate length (L_g). The devices with the δ -doping layers are further studied for two more gate lengths of $0.15\mu m$ and $1.15\mu m$ for optimized results. The drain current (I_d) versus drain voltage (V_d) (drain characteristics) for AlGaAs/AlGaAs/InGaAs (without δ -doping) and AlGaAs/AlGaAs/InGaAs (with δ -doping) PHEMTs at $V_g = -0.6V, -0.4V$ and $0V$ are shown in Fig.4 and Fig.5 respectively. It was observed that the maximum drain current obtained at the bias of $V_d=2V$ and $V_g=0V$ for AlGaAs/AlGaAs/InGaAs PHEMT with δ -doping (391 mA/mm) is more compared to that of

AlGaAs/AlGaAs/InGaAs PHEMT without δ -doping (296 mA/mm) for the gate length $L_g = 0.5\mu\text{m}$. This showed that the introduction of δ -doped layer increased the drain current I_d for zero gate voltage ($V_{gs}=0\text{V}$) and also the channel conductivity.

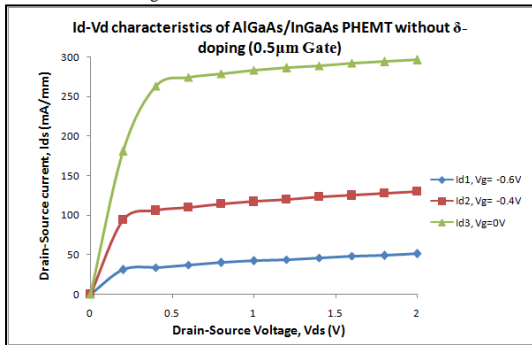


Figure 4: Drain characteristics of AlGaAs/AlGaAs/InGaAs PHEMT without δ -doping ($L_g=0.5\mu\text{m}$)

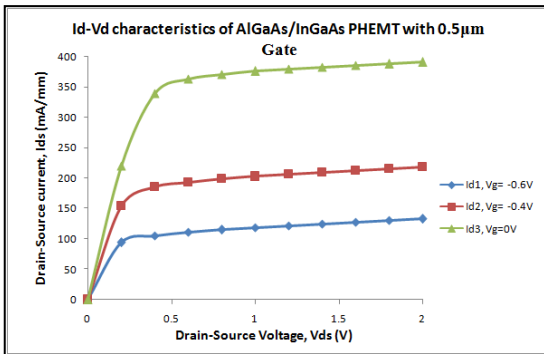


Figure 5: Drain characteristics of AlGaAs/AlGaAs/InGaAs PHEMT with δ -doping ($L_g=0.5\mu\text{m}$)

On increasing the gate length of the δ -doped AlGaAs/InGaAs PHEMT from $0.5\mu\text{m}$ to $1.15\mu\text{m}$, Fig.6, shows that the maximum drain current (I_d) decreases from 391 mA/mm to 351 mA/mm at $V_{gs}=0\text{V}$. But when the gate length is decreased for $0.5\mu\text{m}$ to $0.15\mu\text{m}$, Fig.7, the maximum drain current increases from 391 mA/mm to 428 mA/mm at $V_{gs}=0\text{V}$.

By replacing the AlGaAs barrier layer by InGaP layer increases the maximum drain current (I_d) from 391 mA/mm to 604 mA/mm for $0.5\mu\text{m}$ gate length as shown in Fig.8. Moreover, by changing the gate lengths of InGaP/AlGaAs/InGaAs PHEMT the maximum drain current also changes, 567 mA/mm ($L_g=1.15\mu\text{m}$) and 620 mA/mm ($L_g=0.15\mu\text{m}$), as shown in Fig.9 and Fig.10 respectively.

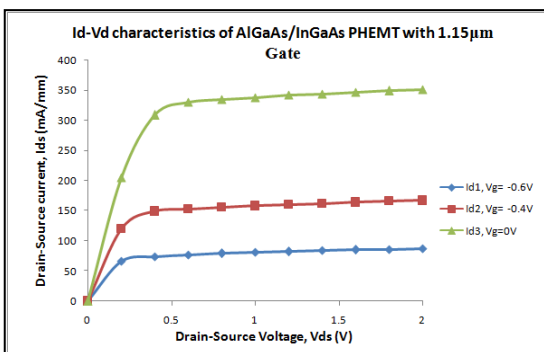


Figure 6: Drain characteristics of AlGaAs/AlGaAs/InGaAs PHEMT with δ -doping ($L_g=1.15\mu\text{m}$)

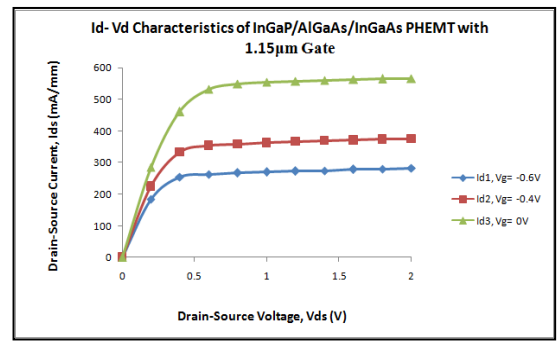


Figure 7: Drain characteristics of InGaP/AlGaAs/InGaAs PHEMT with δ -doping ($L_g=1.15\mu\text{m}$)

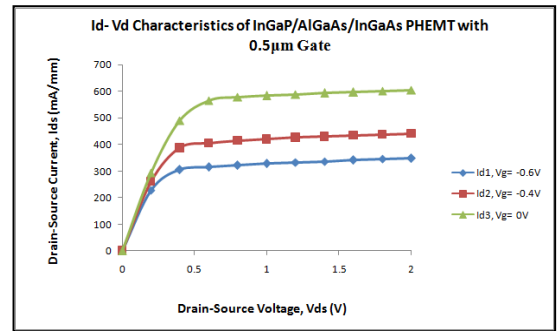


Figure 8: Drain characteristics of InGaP/AlGaAs/InGaAs PHEMT with δ -doping ($L_g=0.5\mu\text{m}$)

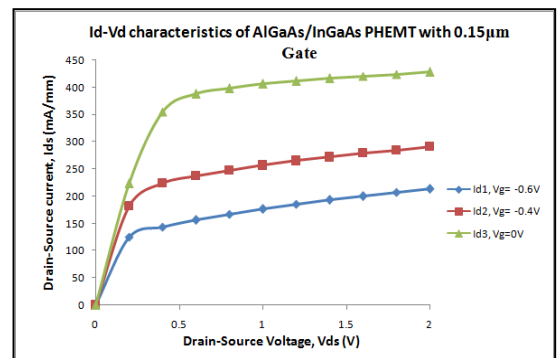


Figure 9: Drain characteristics of InGaP/AlGaAs/InGaAs PHEMT with δ -doping ($L_g=1.15\mu\text{m}$)

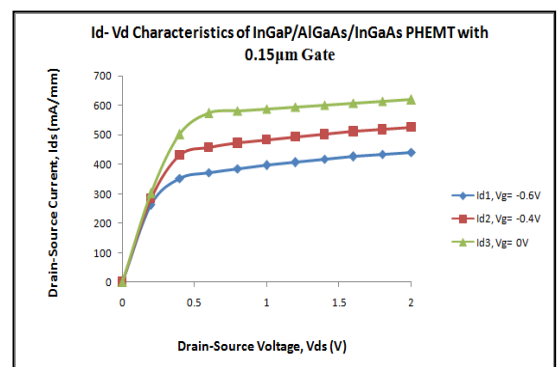


Figure 10: Drain characteristics of InGaP/AlGaAs/InGaAs PHEMT with δ -doping ($L_g=0.15\mu\text{m}$)

The transfer characteristics at $V_d=2\text{V}$ for AlGaAs/InGaAs PHEMT without doping (Fig.11) and different gate lengths of AlGaAs/InGaAs PHEMT with doping (Fig.12, Fig.13, Fig.14)

and InGaP/AlGaAs/InGaAs PHEMT with doping (Fig.15, Fig.16, Fig.17) has been shown .

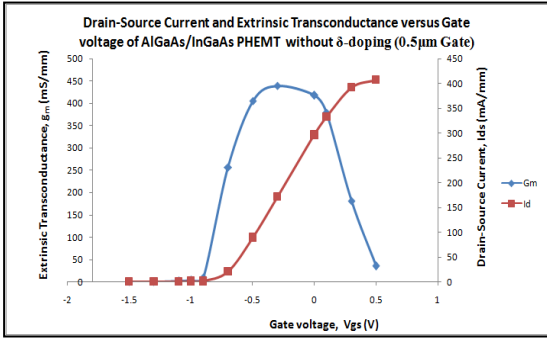


Figure 11: Transfer characteristics of AlGaAs/AlGaAs/InGaAs PHEMT without δ -doping ($L_g=0.5\mu\text{m}$)

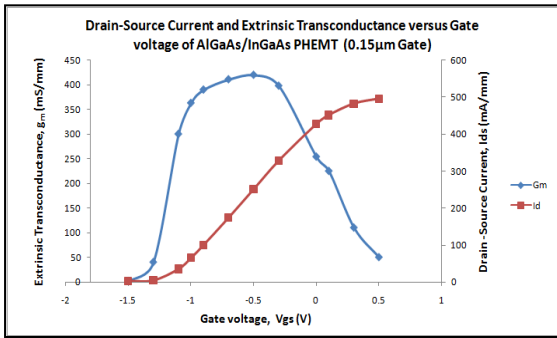


Figure 12: Transfer characteristics of AlGaAs/AlGaAs/InGaAs PHEMT with δ -doping ($L_g=0.15\mu\text{m}$)

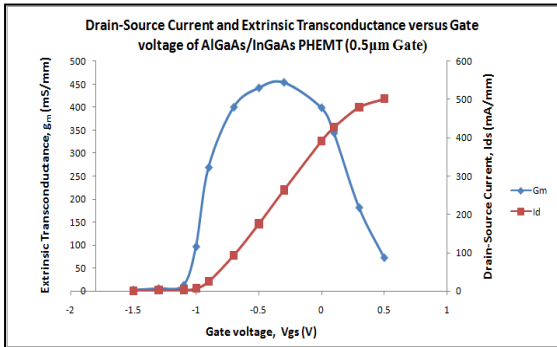


Figure 13: Transfer characteristics of AlGaAs/AlGaAs/InGaAs PHEMT with δ -doping ($L_g=0.5\mu\text{m}$)

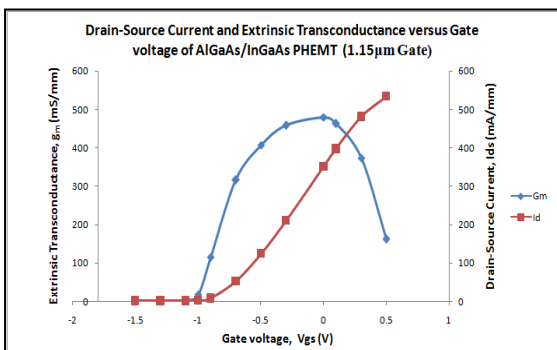


Figure 14: Transfer characteristics Of AlGaAs/AlGaAs/InGaAs PHEMT with δ -doping ($L_g=1.15\mu\text{m}$)

It was observed that the threshold voltage (V_{th}), which is defined as the gate-bias intercept by linearly extrapolating drain current curve from the peak g_m position in transfer characteristics, is nearly -0.8V for AlGaAs/InGaAs PHEMT (without doping), nearly -1V for AlGaAs/InGaAs PHEMT (with doping) and -1.4V for InGaP/AlGaAs/InGaAs PHEMT for $0.5\mu\text{m}$ gate length.

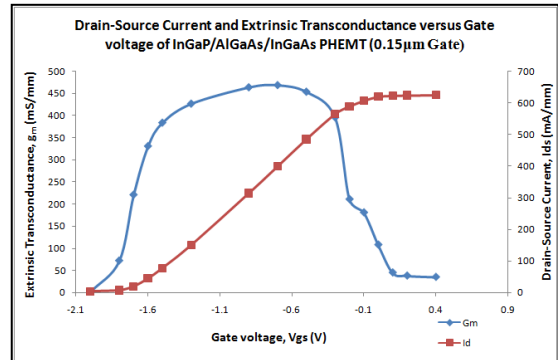


Figure 15: Transfer characteristics of InGaP/AlGaAs/InGaAs PHEMT with δ -doping ($L_g=0.15\mu\text{m}$)

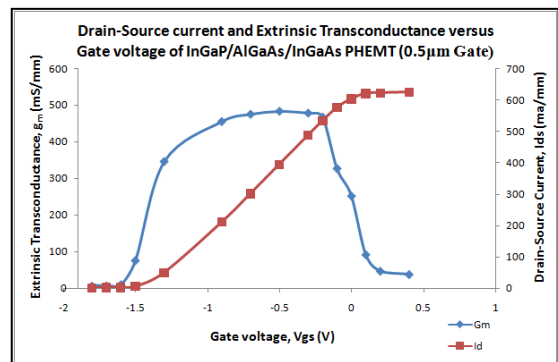


Figure 16: Transfer characteristics of InGaP/AlGaAs/InGaAs PHEMT with δ -doping ($L_g=0.5\mu\text{m}$)

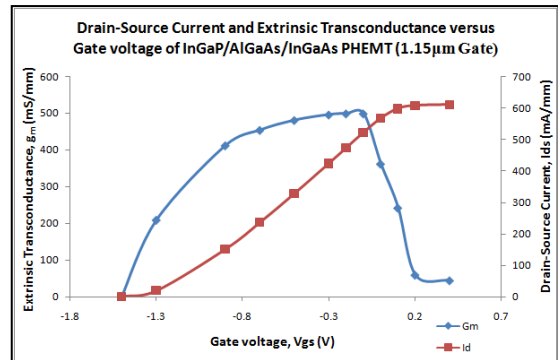


Figure 17: Transfer characteristics of InGaP/AlGaAs/InGaAs PHEMT with δ -doping ($L_g=1.15\mu\text{m}$)

The linearity and maxima of transconductance characteristics increase as the basic PHEMT device is modified with delta-doping and the AlGaAs barrier layer is replaced by the InGaP layer. The transconductance for AlGaAs/InGaAs PHEMT without delta-doping is $G_m=439\text{ mS/mm}$, while for AlGaAs/InGaAs PHEMT with delta-doping

is $G_m=454$ mS/mm and InGaP/ AlGaAs/ InGaAs PHEMT is $G_m=483$ mS/mm.

Table III shows the comparative study of all the three devices with gate length variations. Here, the maximum drain current (I_{dmax}), transconductance (G_m) and the threshold voltages (V_{th}) are observed for InGaP/AlGaAs/InGaAs PHEMT (with δ -doping).

Table III: The Comparative Study Of The Device Parameters Obtained After Simulation

Device Parameters	[Structure I] AlGaAs/ AlGaAs/ InGaAs PHEMT	[Structure II] AlGaAs/AlGaAs/ InGaAs PHEMT (with δ -doping)			[Structure III] InGaP/AlGaAs/ InGaAs PHEMT (with δ -doping)		
	[Lg in μ m]	[Lg in μ m]			[Lg in μ m]		
	0.5	0.15	0.5	1.15	0.15	0.5	1.15
I_{dmax} (mA/mm)	296	428	391	351	620	604	567
G_m (mS/mm)	439	420	454	479	469	483	499
V_{th} (V)	-0.8	-1.2	-1.0	-0.8	-1.7	-1.4	-1.3

Lg = Gate Length (0.15 μ m, 0.5 μ m and 1.15 μ m)

IV. CONCLUSIONS

In this paper three PHEMT devices have been simulated and it is observed that the performance for InGaP/AlGaAs/ InGaAs double delta-doped structure is much better due to better carrier confinement since the Al which reaction prone is absent in the barrier layer. As a result, the conductivity of the channel increases showing maximum drain current (I_{dmax}) of 604 mA/mm for 0.5 μ m. Also, as the gate length is reduced,

the maximum drain current increases. Moreover it is also observed that the transconductance of this device is higher ($G_m=483$ mS/mm) as compared to the other two device structures. So, the delta doped layer and the InGaP material as barrier layer improve the performance of the device.

References

- [1] B. R. Nag, Physics of Quantum Well Devices, Kluwer Academic publishers, 184-185 (2002).
- [2] D. Delagebeaudeuf and N. Linh, "Metal-(n) AlGaAs-GaAs two-dimensional electron gas FET", IEEE Trans. On Electron Devices, **29**, 955-960 (1982).
- [3] J. P. Collinge and C. A. Collinge, Physics of Semiconductor Devices, Kluwer Academic publishers, 321-324 (2005).
- [4] S. M. Bahauddin, M. A. B. Aziz and Z. H. Mahmood, "100nm-gate matched InAlN/AlN.GaN HEMT for high power giga hertz frequency application", Journal of Electron Devices, **14**, 1118-1121 (2012).
- [5] G. Raj, H. Pardeshi, S.K. Pati, N. Mohankumar, C. K. Sarkar, "Physics based charge and drain current model for AlGaIn/GaN HEMT devices", Journal of Electron Devices, **14**, 1155-1160 (2012).
- [6] M. Missous, A. A. Aziz, and A. Sandhu, "InGaP/InGaAs/GaAs high electron mobility transistor structure grown by solid source molecular beam epitaxy using GaP as phosphorous source", Japanese Journal of Applied Physics, **36**, 647-649 (1997).
- [7] F. E. G. Guimaraes, B. Elsner, R. Westphalen, B. Spangenberg, H. J. Geelen, P. Balk, and K. Heime, "LP-MOVPE growth and optical characteristic of InGaP/GaAs heterostructure: Interface, quantum wells and quantum wires", Journal of Crystal Growth, **124**, 199-206 (1992).
- [8] K.Jang, J. Lee, J. Lee and K. Seo, "In_{0.49}GaP/Al_{0.45}GaAs barrier enhancement-mode pseudomorphic high electron mobility transistor with high gate turn-on voltage and high linearity", Japanese Journal of Applied Physics, **45**, 3355-3357 (2006).
- [9] H. Q. Zheng, S. F. Yoon, B. P. Gay, K. W. Mah, K. Radhakrishnan, and G. I. Ng, "Growth optimization of InGaP layers by solid source molecular beam epitaxy for the application of InGaP/In_{0.2}Ga_{0.8}As/GaAs high electron mobility transistor structures", Journal of Crystal Growth, **216**, 51-56 (2000).